Integrative Biology

Accepted Manuscript

This article can be cited before page numbers have been issued, to do this please use: S. Chandrasekaran, H. Deng and Y. Fang, *Integr. Biol.*, 2015, DOI: 10.1039/C4IB00298A.

ROYAL SOCIETY OF CHEMISTRY

www.rsc.org/ibiology

Integrative Biology

Integrative Biology

Dynamic Article Links ►
View Article Online
DOI: 10.1039/C4IB00298A

Cite this: DOI: 10.1039/c0xx00000x

www.rsc.org/Integrative Biology

Paper

PTEN deletion potentiates invasion of colorectal cancer spheroidal cells through 3D Matrigel

Siddarth Chandrasekaran,[a,b] Huanyun Deng,[a] and Ye Fang[a,*]

Received (in XXX, XXX) Xth XXXXXXXXX 20XX, Accepted Xth XXXXXXXXX 20XX
DOI: 10.1039/b000000x

PTEN (phosphatase and tensin homolog), a tumour suppressor negatively regulating the PI3K signalling pathway, is the second most frequently mutated gene in human cancers. Decreased PTEN expression is correlated with colorectal cancer metastases and poor patient survival. Three dimensional (3D) multicellular spheroid models have been postulated to bridge the gap between 2 D cell models and animal models for cancer research and drug discovery. However, little is known about the impact of PTEN deletion on the invasion of colon cancer spheroidal cells through 3D extracellular matrix, and current techniques are limited in their ability to study in vitro 3D cell models in real-time. Here, we investigated the migration and invasion behaviours of the colon cancer cell line HCT116 and its PTEN-/- isogenic cell line using three different in vitro assays, wound healing, Transwell invasion, and label-free single cell 3D^2 invasion assays enabled by resonant waveguide grating (RWG) biosensor. Light microscopic and RWG imaging showed that PTEN deletion influences the spheroid formation of HCT116 cells at high seeding density, and accelerates the spontaneous transfer from the spheroid to substrate surfaces. In vitro migration and invasion assays showed that PTEN knockout increases the 2D migration speed of HCT116 cells, and the invasion rate of individual cells through Matrigel or cells in spheroid through 3D Matrigel; moreover, PI3K inhibitor treatment drastically reduces the invasiveness of both cell lines. This study suggests that PTEN knockout potentiates the invasiveness of colorectal cancer spheroidal cells through 3D extracellular matrix, and label-free single cell assay is powerful for investigating cancer cell invasion, in particular using 3D cell models.

Insight, innovation, integration

Cell invasion is mostly studied using 2D cell models in vitro; and these 2D assays have shown that RNAi knockdown of PTEN increases migration and invasion capacities of colorectal cancer cells. Here we demonstrated that RWG biosensor permits label-free, real-time and single cell quantification and mechanistic study of the PTEN deletion increased invasion of spheroidal colon cancer cells through 3D matrigel.

Introduction

The lipid phosphatase PTEN (phosphatase and tensin homolog) is a tumour suppressor that is under-expressed in many human cancers arising from deletions, mutations or gene silencing.[1,2] PTEN functions as a negative regulator of class I phosphatidylinositol 3-kinases (PI3K) via dephosphorylation of phosphatidylinositol-3,4,5-trisphosphate, which is a potent activator of 3-phosphoinositide-dependent kinase (PKD) and AKT.[3] Loss of PTEN thus leads to hyperactivation of PI3K pathway. PTEN is one of the most frequently mutated genes in human cancers including colorectal cancers (CRCs).[4] The prevalence of PTEN mutations in CRCs varies between 1% and 29%,[5,6] while PTEN deletion was found to be in approximately 20-49% of CRCs, the median being 40%[7-9]. Loss of PTEN is more prevalent in later stage CRCs, and is high as approximately 83% of metastatic CRCs.[10] Loss of PTEN has been also reported to be associated with increased cancer cell motility and invasiveness, and poor overall patient survival.[11] These findings suggest that loss of PTEN may provide an environment for the migration, invasion and the subsequent metastasis of CRCs.

Cancer metastasis from the primary site to distant organs is the main cause of cancer related death.[12] The haematogenous metastatic cascade is an orchestrated multi-step process in which cells from the primary tumour invade the surrounding tissue and enter the peripheral circulation.[13] The cells that survive from the fluid shear stress and immune cells in the circulation can extravasate and form metastases at distant sites.[14] The metastatic cascade is regulated by multifarious interactions between tumour cells and other cells in the tumour microenvironment.[15,16] These interactions play an important role in determining the fate of a cell that leaves the primary tumour. Amassing data, in particular

View Article Online
DOI: 10.1039/C4IB00298A

Cite this: DOI: 10.1039/c0xx00000x

www.rsc.org/Integrative Biology

Paper

genomic landscape studies, have shown that human cancer is a pathway dysregulated disease, since tumour-associated genes and their mutations are mostly enriched in signaling proteins involved in a small number of pathways.[4,16,17] The dysregulation of PI3K pathway is common in many human cancers including CRCs[4] and occurs through somatic activating mutations in class IA PI3Ks, most frequently PIK3CA,[18,19] or through PTEN inactivation. PI3K pathway is central to the control of cell growth, proliferation and adhesion-dependent survival.[20,21] Dysregulation of the PTEN-PI3K may cause loss of epithelial characteristics, increase the possibility of cells acquiring mesenchymal properties and cell motility and invasiveness.[3] However, studying the role of the PTEN-PI3K pathway in CRC invasion is sparse in literature and mostly relies on conventional *in vitro* two-dimensional (2D) cell models. It has been reported that somatically mutated PI3KCA occurs in over 25% of CRCs[18] and promotes invasion of colon cancer cell lines through Matrigel using Transwell assay[22]. RNAi knockdown of PTEN was found to induce epithelial-mesenchymal transition (EMT) in human CRC cells, and increase the invasion and migration of CRCs using 2D wound and Transwell assays.[23,24] EMT is a critical early event in the invasion and metastasis of many cancers.[25]

In vitro tumour assays have seen a radical shift from 2D to 3D in the past years.[26-29] This is mostly due to increasing evidence suggesting that compared to 2D monolayer cell culture models, 3D multicellular spheroidal models more closely recapitulate the *in vivo* situation of solid cancers, thus permitting more accurate prediction of *in vivo* drug efficacy, potency and safety.[30] These 3D models have been reported to have better predictive power for cancer cell growth,[31] invasive potential,[32] and drug responsiveness,[33,34] and more closely mimic the phenotypic heterogeneity[35,36] and microenvironments of tumors[37]. Coincident with the increasing use of 3D spheroidal cell models for cancer research is the development of advanced invasion and migration assays.[38] Spheroid sprouting assay is useful to study the invasion of cells in 3D spheroid into surrounding 3D extracellular matrix (ECM) structure.[39,40] However, this assay requires imaging techniques to track the shape and location of cells in a 3D matrix, and mostly detects late invasion events since imaging is limited to visualize the outer border of spheroids placed in the gel. Cell invasion into spheroid assay is useful to investigate the ability of a first cell type, either in isolation[41] or in a spheroidal structure[42,43], into the spheroidal cluster of a second cell type. However, this assay often uses fluorescently labelled cells, have low temporal resolution, and poses difficulty in the quantification of invading cells.[38]

Recently, we reported the development of a label-free, real-time, single-cell, and quantitative assay to monitor the invasion of 3D spheroidal cells through a 3D matrix[44]; this assay is termed single-cell 3D^2 invasion assay. Central to this assay is to use a label-free resonant waveguide grating (RWG) biosensor to monitor the adhesion of cells after dissociated from a single spheroid and invaded through a 3D ECM (e.g., Matrigel) (**Fig.1**).

Here, uniform spheroids of a cancer cell type are generated by culturing equal number of cells in a 96-well ultralow-attachment (ULA) round-bottom microplate. The ULA plate enables the self-assembly of cancer cells into a single 3D spheroidal cluster in the bottom of each well mediated by surface chemistry and gravity force.[45] A layer of 3D Matrigel film is formed on the biosensor surface through gelation of Matrigel at 37^{o}C overnight. Matrigel is a solubilized basement membrane preparation extracted from mouse sarcoma, a tumour rich in ECM proteins, and is the most commonly used ECM for investigating the invasiveness of cancer cells. The 3D/3D invasion process is monitored in real-time using a RWG imager with a spatial resolution of 12μm and a temporal resolution up to 3sec.[46,47] The RWG biosensor is centred on waveguide nano-grating arrays embedded in standard microtiter plates for real-time monitoring of receptor signaling and drug pharmacology in native cells[48-56].

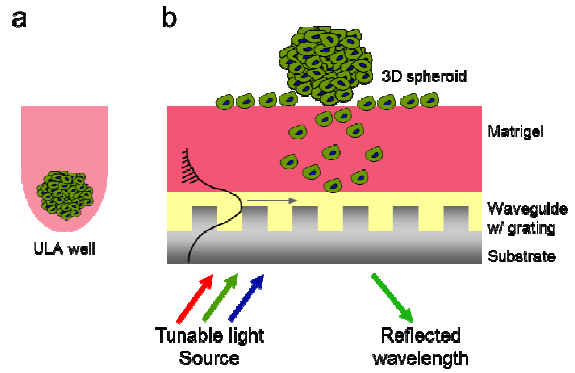

Fig.1 Schematic drawing of label-free single cell 3D^2 invasion assay. (a) Spheroids of cancer cells are formed in ultralow-attachment round-bottom microplate. (b) Once placed onto 3D ECM (e.g., Matrigel) coated biosensor, some cells in the spheroid start to dissociate and adhere onto the top surface of the coating with a characteristic spontaneous transfer rate. Some of these adhered cells then invade through the 3D ECM and ultimately reach the sensor surface, leading to a dynamic mass redistribution (DMR) signal arising from cell adhesion as monitored in real-time at single cell level using a resonant waveguide grating imager. The DMR signal is recorded as the shift in resonant wavelength in picometer (pm).

Here we set to determine the impact of PTEN deletion on the growth pattern into a spheroidal structure of a colorectal cancer cell line HCT116, the spontaneous transfer rate from the spheroidal structure to different surfaces, and the invasion rate through 3D Matrigel coating of two different densities. Instead of typical RNAi knockdown,[23,24] we compare the behaviour of a pair of isogenic cell lines, wide type HTC116 (HCT116-WT) and its PTEN null cell line (HTC116 PTEN-/-). We further determine the ability of the label-free invasion assay to be used in investigative studies involving early drug discovery and testing.

Materials and methods

Materials

Dynamic Article Links ►
View Article Online
DOI: 10.1039/C4IB00298A

Cite this: DOI: 10.1039/c0xx00000x

www.rsc.org/Integrative Biology

Paper

LY294002 and wortmannin were obtained from Tocris (St. Louis, MO, USA). Epic® 384-well biosensor cell culture compatible microplates, ULA 96-well round bottomed plates (Catalog #7007), flat bottom 96-well plates, and Corning® Matrigel® Growth Factor Reduced (GFR) Basement Membrane Matrix (Catalog #354230) were obtained from Corning Incorporated (Corning, NY, USA). The Matrigel as received consists of approximately 60% laminin, 30% collagen IV, and 8% entactin. Entactin is a bridging molecule that interacts with laminin and collagen IV, and contributes to the structural organization of these ECM molecules. Matrigel generally contains transforming growth factor-β (TGF-β), epidermal growth factor, insulin-like growth factor, fibroblast growth factor, tissue plasminogen activator, and other growth factors which occur naturally in the EHS tumour. However, the Matrigel used has a reduced level of a variety of growth factors except for TGF-β. The isogenic colorectal carcinoma cell lines, HCT116-WT and HCT116-PTEN-/- cells were licensed to Corning Incorporated from Horizon Discovery Ltd. (Cambridge, UK).

Cell culture and spheroid formation

Both cell lines were cultured in McCoy's 5A medium (Catalog #16600, Life Technologies, Carlsbad CA, USA) supplemented with 10% fetal bovine serum (FBS), 4.6g/L glucose, 1.5mM glutamine and 1% penicillin and streptomycin. These cells were grown in T-75 flask at 37°C with 5% CO_2 and were passaged or used for experimental culture when approaching 90% confluence. For tumour spheroid culture, 200µL cell suspension with varied number of cells per well was added to each well in an ULA round-bottom 96well microplate. At day 3 in culture, 100µL of old media was removed and 100µL of fresh media was added. After cultured in ULA plate for five days the resultant spheroids were used in invasion and migration assays. To minimize disruption of the spheroids during media changes the pipette tip was held at approximately a 45° angle away from the center of the well bottom.

3D Matrigel formation

We used Matrigel as the model for cell invasion assays. Matrigel is a liquid at 4°C and start to form a gel above 10°C.[57] To prevent premature gelation, Matrigel, the biosensor plates, Transwell inserts, pipets, and tips all were pre-cooled during the preparation step. To coat Transwell, the Matrigel received was diluted to a final concentration of 0.1mg/mL and 100µL of the diluted Matrigel® was pipetted into the Corning HTS Transwell® 24 Well Permeable Supports with transparent polycarbonate membrane containing 8µm sized pores (Catalog #3397, Corning) and allowed to gel overnight.

To form 3D gel on biosensor surface, the Matrigel was first diluted using McCoy's 5a Medium Modified containing 10% FBS, 1x Pennstrep to 0.1mg/mL at 4°C. 20µl the diluted solution was then added to each well of a 384well biosensor microplate at 4°C. Afterwards, the microplates were incubated inside an incubator at 37°C under air/5% CO_2 for 24hrs.

Light microscopic imaging

The cell morphology was examined using an inverted light microscope (Nikon Eclipse TS100 equipped with NIS Elements F3.0 Software, Nikon Instruments Inc., Melville, NY, USA). Data process and analysis were performed using NIH Image J (http://imagej.nih.gov/ij/).

Wound healing assay

The wound healing assay, also known as scratch recovery assay, is a classical 2D cell migration assay to determine the migratory behaviour of cells, which is reflected by the rate of recovery of the scratched region.[58] Cells were grown to confluency in a 6-well plate (Corning). The confluent cells were serum starved overnight by incubating with culture medium without serum. A scratch was made with a sterile 200µL pipette tip in a marked region of the well. There were three wells for each cell line and images of the marked scratch were taken immediately after inducing the scratch. The wells with scratches were incubated in serum free medium at 37°C with 5% CO_2. The recovery of the scratch was determined by imaging the same field 48hrs later and built-in ImageJ drawing options were used to determine the scratch area and percentage of reduction in wound size. The data reported are the average of five different fields for each cell type.

Transwell invasion assay

The Matrigel coated Transwell invasion assay was performed to determine the invasive potential of cells. The coated transwell inserts are termed invasion chambers. This assay is an endpoint assay to monitor the invasion of cells in isolation through 3D Matrigel. Specifically, cells were dissociated in serum free media and 100µL of cell suspension with a density of $2.5x10^4$cells/mL was plated in the invasion chamber. The invasion chambers were then transferred to 24-well plate filled with 750µL of cell culture media with 5% FBS as a chemo attractant. Equal numbers of uncoated transwell inserts were prepared as a control. The cell invasion chambers were incubated for 24hrs at 37°C with 5% CO_2. After incubation, the chambers were removed and washed twice with PBS and the non-invading cells were discarded using a cotton swab moistened with culture media. The cells were fixed in 4% paraformaldehyde, permeabilized in 100% methanol and stained using crystal violet stain and the number of invading cells were manually counted using a light microscope. The percentage invasiveness was calculated by normalizing the number of invading cells in Matrigel coated inserts with the number of invading cells in uncoated (control) inserts. The invasion rate reported is the average of five different invasion chambers.

Label-free $3D^2$ invasion assays

The $3D^2$ invasion assays were performed using a high resolution version of Epic® benchtop BT system (Corning).[46,47] This system is capable of simultaneously imaging an array of 3x4 biosensors

View Article Online
DOI: 10.1039/C4IB00298A

Cite this: DOI: 10.1039/c0xx00000x

www.rsc.org/Integrative Biology

Paper

within a Corning Epic 384-well microplate, and uses a complementary metal oxide semiconductor (CMOS) digital camera to record resonant wavelength images with a spatial resolution of 12µm and temporal resolution up to 3sec. To reduce the size of data generated, a temporal resolution of 1min was used for the $3D^2$ assay. The entire assay was performed inside a typical cell culture incubator at 37°C and 5% CO_2.

The $3D^2$ invasion assay was done in two steps. First, the Matrigel coated microplates were incubated for 30 minutes on Epic imager until all sensors reached a steady baseline. Second, the invasion through Matrigel was monitored by transferring tumour spheroids onto the Matrigel coated microplates. All spheroids used for invasion assays were generated by seeding 1000 cells per well into a 96-well round-bottom ULA surface and cultured for five days. The transfer was performed using wide-bore tips to ensure that spheroids were not dissociated during the transfer. In some cases, two tumour spheroids were transferred on a single well to increase the probability of placing spheroids within the biosensor area. The time series DMR images were collected continuously for 24hrs. For performing PI3K inhibitor studies, 10µL 10 µM LY294002 and wortmannin was added to each well of the microplate prior to the transfer of tumour spheroids, so the final effective concentration was 2.5µM. Equal number of wells was also added with appropriate vehicle controls. The microplates were left on Epic imager for 60 minutes to reach steady baseline before transferring the tumour spheroids.

Statistical analysis

DMR data were analysed using GraphPad Prism 6.0 (GraphPad Software Inc., San Diego CA, USA). The pixelated data were extracted using Corning Epic processor software and were further processed using functions in Microsoft Excel (Microsoft Inc., Seattle WA, USA). The statistical significance reported was tested using student's t-test for most assay results, except for Bonferroni's multiple comparison test used for drug effects with the Prism 6.0.

Results and Discussion

To investigate the role of PTEN in the invasiveness of CRCs, we use three distinct assays, 2D wound, Transwell, and label-free $3D^2$ invasion assays, to compare the behaviour of HCT116-WT with HCT116-PTEN-/- cells. HCT116 is a microsatellite-unstable and metastatic human CRC cell line, and can grow in multilayer but is incapable of polarization or intestinal epithelial differentiation.[24] The PTEN-/- line is directly derived via homologous knockout of PTEN in HCT116 by deletion of exon 5 which encodes active site of the protein.[59] The wide-type cell line does not bear any somatic PTEN mutations, but has an H1047R mutation of PI3KCA in exon 20 (kinase domain).[22]

PTEN deletion influences spheroid formation and growth

We first investigated the influence of PTEN deletion on the formation and growth of multicellular spheroid in ULA round-bottom microplate using three different seeding densities. Results showed that when the seeding density was at 1000 cells per well, the two cell lines exhibited indistinguishable growth patterns; that is, cells were loosely attached right after seeding, started forming irregular clusters at day 1, and spheroids at day 3, which continuously grown in size (**Fig.2a-k**). This result suggests that under translational spheroid formation condition PTEN knockout has little impact on the formation and growth of spheroids.

However, distinct patterns were observed when the seeding density was increased to 20,000 or 30, 000 cells per well (**Supplementary Fig.S1; Fig.2l-m**). Under both seeding conditions, the wide-type cells already formed spheroids at Day 1, but their sizes were continuously decreased to day 4. In contrast, the PTEN-/- cells formed a spheroid whose size was barely changed over the four day culture. The compaction of large aggregates of the wide-type cells into a stable spheroid is consistent with the fact that cell-cell interaction promotes compaction. However, loss of PTEN is known to cause loss of epithelial characteristics,[3] thus preventing the compaction of large cell aggregates and leading to a loosely packed spheroid. Furthermore, the inability of these large spheroids of both cell lines to continue growing is likely due to the limitation of nutrition and oxygen supply and/or accumulation of cell metabolic waste (e.g., lactate).[60,61] Nonetheless, the different spheroid formation patterns of the two cell lines are intriguing and worthy of further investigations.

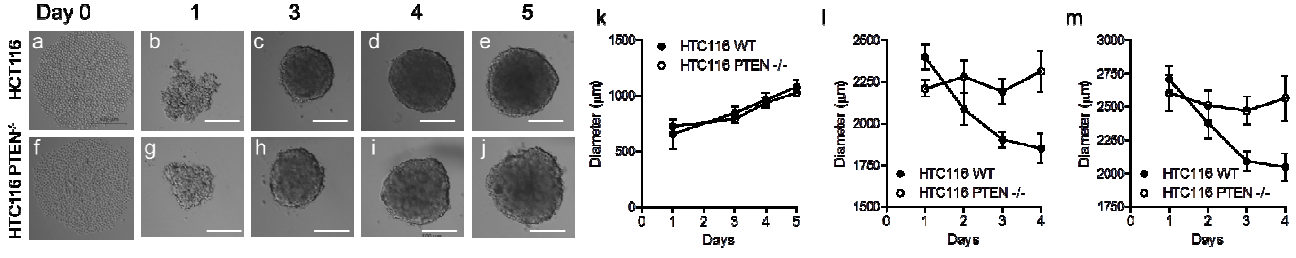

Fig. 2 Growth pattern of spheroidal cells in 96-well round-bottom ULA surface. Seeding density: 1000 cells per well (a-k); 20000 cells per well (l), or 30000 cells per well (m). (a-j) light microscopic images, Scale bar: 500µm. (a-e) HCT116 WT cells at Day 0 to Day 5. (f-j) HCT116-PTEN-/- cells at Day 0 to Day 5. (k-m) The diameter of spheroids of both cell lines as a function of culture duration.

Dynamic Article Links ►
View Article Online
DOI: 10.1039/C4IB00298A

Cite this: DOI: 10.1039/c0xx00000x

www.rsc.org/Integrative Biology

Paper

Data in (k-m) represents mean±s.d. (n=5).

Considering that it is important to have spheroids that are much smaller than the dimension of the biosensor (2x2 mm) for effectively positioning and monitoring invasion through a 3D matrix on the biosensor surface, we only used the spheroids obtained using five day culture of 1000 cells per well for spheroidal cell invasion studies.

PTEN deletion increases 2D migration rate of HCT116 cells

Motility is one of the key hallmarks of a metastatic cancer cell. To determine the role of PTEN deletion in the migration of the CRC cells we used 2D wound healing assay to quantify the differences between the two cell lines under serum-free condition. Results showed that by the end of 48hrs the PTEN-/- cells increased the recovery rate by 2.93 fold, compared to the parental line (**Fig.3a**), suggesting that the PTEN deletion increases the migratory potential of HTC116 cells.

PTEN deletion increases invasion rate of isolated CRC cells through 3D Matrigel

Next, we used Matrigel transwell assay to quantify the impact of PTEN deletion on the invasive potential of HCT116 cells. This assay measures the invasion of individual cells through Matrigel coated substrates having defined micropores, and is an end-point measurement of invasion. This assay mimics local invasion of tumour cells through the ECM or basement membrane. The invasiveness was quantified by counting the number of invaded cells and normalizing to those in uncoated transwell inserts. Results showed that there was 1.24 fold higher numbers of the PTEN-/- cells invaded through the matrix than the parental line, when serum media was used as the chemo-attractant (**Fig.3b**). This result suggests that PTEN deletion increases the invasiveness of the CRC cells.

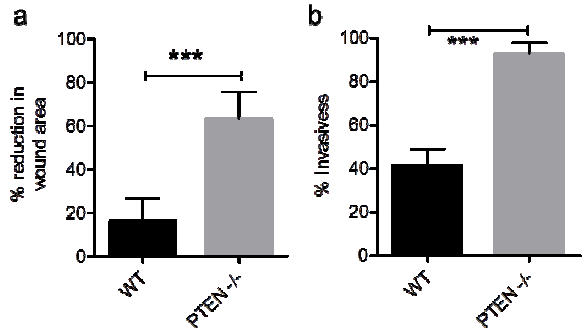

Fig.3 The 2D migration rate (a) and the invasion rate through Matrigel coated Transwell (b) of HCT116 *versus* HCT116-PTEN-/- cells. Data represents mean±s.d. (n=5). *** p<0.001.

PTEN deletion accelerates the transfer of CRC cells from the spheroid to biosensor and 3D Matrigel surfaces

Next, we used light microscopic and RWG imaging techniques to examine the spontaneous behaviour of CRC cells after the spheroids were placed on to the top surface of three different substrates: uncoated, low (0.1mg/ml) and high (0.2mg/ml) Matrigel coated biosensor surfaces (**Fig.4, Supplementary Fig.S2**). After one day label-free real-time monitoring of the spheroid on a sensor, a DMR image was first obtained, and a light microscopic image was then acquired. RWG DMR imaging has a short penetration depth (~200nm) away from the waveguide thin film;[49] however, light microscopy has a much thicker imaging depth. With 20µl Matrigel solution used for the coating, the height of resulted 3D matrix coating was estimated to be 1.2mm.[44] Thus, on the uncoated (bare) surface RWG imaging directly examines the adhesion pattern of cells after spontaneously dissociated from the spheroidal structure. However, on the coated surfaces RWG imaging only examines cell adhesion on the biosensor surface, (that is, right below the 3D coating), after dissociated from the spheroid and invaded through the matrix. Of note, the spheroid itself obviously obscures the accurate light microscopy imaging of adherent cells when the adhesion area is smaller than the cross-section of the spheroid.

Light microscopic and RWG imaging showed that 24hrs after a spheroid was placed onto the bare surface the parental line gave rise to an adhesion area that was 63% of the cross-sectional area of the starting spheroid (comparing **Fig.4a** with **Fig.4c**); however, the PTEN-/- cells gave rise to an adhesion area that was 102% of the cross-sectional area of the starting spheroid (comparing **Fig.4b** with **Fig.4d**). PTEN deletion significantly increased the spontaneous dissociation and subsequent adhesion onto the bare sensor surface (**Fig.4e**).

DMR single cell analysis further supports this conclusion. Given that the size of spheroids is much smaller than the dimension of each sensor, an intra-sensor referencing was used to eliminate any artefacts associated with mismatch in temperature and bulk index during the spheroid placement step. To do this, a sensor was divided into a background zone (that is, the cell free area indicated by the white circular dotted line) and a cell adhesion zone (indicated by the black circular dotted line) in **Fig.4c**. The averaged responses of both zones were first obtained, and then subtracting the background signal from the cell adhesion signal led to the background-free response arising from cell adhesion (**Supplementary Fig.S3**). Similarly, subtracting the background signal from the response at each pixel led to the net response arising from cell adhesion at the respective pixel (**Fig.4f-g**).

For single pixel/cell analysis, the time series DMR images were obtained after the starting resonant wavelengths at all pixels were normalized to zero. The initial adhesion point, designed as the coordinate of (0,0), was identified as the pixelated location at which the first positive DMR occurrs. For the bare surface this

View Article Online
DOI: 10.1039/C4IB00298A

Cite this: DOI: 10.1039/c0xx00000x

www.rsc.org/Integrative Biology

Paper

location is approximately the initial contact point of the spheroid with the surface, wherein the cell has the shortest path to adhere onto the surface. Results showed that the contact of a spheroid of the parental cells with the bare surface over 24hrs led to a time-dependent expansion of a circular adhesion area, as evidenced by representative pixelated DMR along the horizontal dot line of Figure 4c (**Fig.4f**). The closer the pixelated location to the initial adhesion point is, the faster the DMR occurs. Furthermore, the adhesion DMR at all pixels consist of three phases, a rapid increasing phase followed by a rapid decaying phase to a level slightly above the baseline, and a slowly increasing phase to a moderate level till the end of the assay. This characteristic suggests that the CRC cells adhere onto the surface rapidly but weakly, as well as actively remodel the surface.

Similar trend was observed for the PTEN-/- cells, but with different characteristics (**Fig.4g**). First, at the end of the assay the PTEN knockout cell line led to significantly higher number of adhesion events than the parental line did (**Fig.4h**). The adhesion events were calculated based on the number of pixels whose DMR amplitude is greater than 200pm at the end of assay. Second, PTEN deletion accelerated the occurrence of cell adhesion events, as evidenced by the distribution of the time to reach 200pm (that is, an adhesion event) (**Fig.4i**). These results further confirm that PTEN knockout increases the spontaneous transfer of CRC cells from the spheroidal structure to the bare surface.

Similarly, light microscopic imaging showed that PTEN deletion also increased the spontaneous transfer rate of CRC cells from the spheroid to the top surfaces of both low and high Matrigel coatings, although the coating was found to further significantly increase the transfer rate (**Supplementary Fig.S2**).

Together, these results showed that PTEN deletion increases the spontaneous transfer and subsequent adhesion of CRC cells in spheroid onto distinct surfaces including ECM.

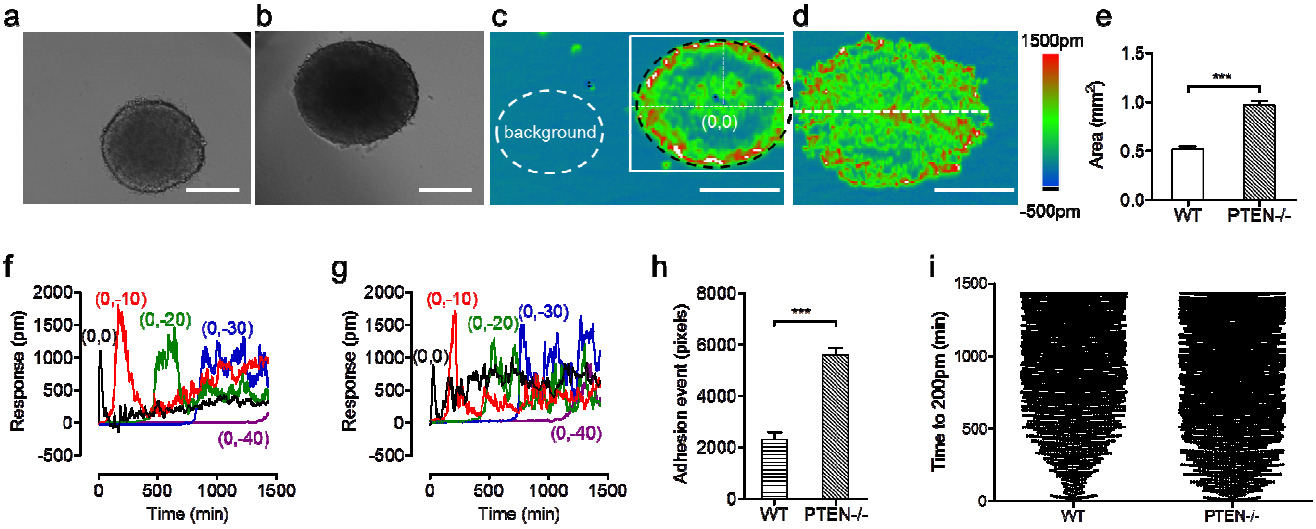

Fig. 4 PTEN deletion increases the spontaneous transfer of cells in spheroid to the bare biosensor surface. (a, b) Light microscopic image of the wide-type (a) or PTEN-/- cells (b). (c, d) Corresponding DMR image of the wide-type (c) or PTEN-/- cells (d). Scale bar for (a-d): 500μm. False colour bar for (c, d): -500 to 1500pm. All images were obtained 24hrs after the spheroid was placed onto the surface. (e) The adhesion area at 24hrs *versus* cell types. (f) The representative real-time DMR of the wide-type cells at single pixelated position along the dotted line indicated in (c). (g) The representative real-time DMR of the PTEN-/- cells at single pixelated position along the dotted line indicated in (d). (h) The total adhesion events at 24hrs *versus* cell types. (i) The distribution of the adhesion time to reach 200pm *versus* cell types. Data represents mean±s.d. for e, h, i (n = 3). *** $p<0.001$.

PTEN deletion increases the invasion kinetics of CRC cells in spheroid through 3D Matrigel at single cell level

Next, we examined the effect of PTEN knockout on the kinetics of the invasion and adhesion of CRC spheroidal cells through the 3D Matrigel of two different densities at single cell level. RWG imaging showed that compared to the bare surface, Matrigel coating slowed down the adhesion onto the sensor surface in an ECM density dependent manner for both cell lines (**Supplementary Fig.S2**). This suggests that cells have to dissociate from a spheroid, invade through the 3D matrix before they can adhere onto the sensor surface; and the higher density Matrigel is the slower the invasion is. Furthermore, the PTEN-/- cells generally gave rise to a greater adhesion area after invasion through the coating than the wide-type cells did (**Supplementary Fig.S2**), suggesting that PTEN deletion increases the invasion of CRC cells in spheroid through the 3D Matrigel. Of note, for both cell lines the adhesion area on the top surface of the coating, as observed using light microscopy, was much larger than that on the sensor surface, as measured with RWG imager

View Article Online
DOI: 10.1039/C4IB00298A

(**Supplementary Fig.S2**), suggesting that once dissociated from the spheroid cells preferably travel along the top surface of the gel over the invasion through the 3D matrix. This is consistent with the notion that the migrating cells are believed to preferably take the route of least resistance.[38]

For single cell analysis, the intra-sensor referencing approach was used again to correct the background. Similarly, the initial adhesion point was also identified, as the pixel where a single cell invades through the matrix and reaches the sensor surface, leading to the first adhesion DMR. For spheroids on the 3D matrix the initial adhesion point also approximates very closely to the initial contact point of the spheroid with the top surface of the matrix, where the cell has the shortest distance to invade through the matrix. For better view, only the DMR of representative pixels for each condition were showed (**Fig.5a-d**). Results showed that the DMR characteristics on the coated surfaces were distinct from those on the bare surface. First, compared to the rapid rise and decay on the bare surface, the DMR on the coated surfaces were generally more sustained over the entire day. Second, the maximal DMR amplitudes were generally smaller on the coated surface than those on the bare surface. Third, the DMR were smoother on the coated surface than those on the bare surface. Fourth, in general the later a DMR occurs the smaller the slope is to reach its immediate maximal. All these characteristics seem to be insensitive to the cell lines and matrix density. These behaviours are best explained by that the invading cells need take extra time to reach optimal adhesion, and the presence of 3D matrix seems limit the movement of the cells once contacted with the sensor surface.

To further understand the mechanism of cells invading through the matrix and adhering onto the sensor surface, we performed the location-dependent analysis. This was done by calculating the lateral distance of all pixels from the initial adhesion point, as well as the time required to reach 200pm positive DMR response for each pixel when applicable. Although it is difficult to determine the exact path of invading cells within the matrix, we reasoned that the lateral distance is a useful parameter to investigate the invasion behaviour of spheroidal cells owing to the fact that all cells need invade through the same 3D matrix.[44] On the other hand, the adhesion time mostly reflect the time required for a cell to invade through the matrix and arrive at the sensor surface, considering the rapid kinetics of cell adhesion itself.

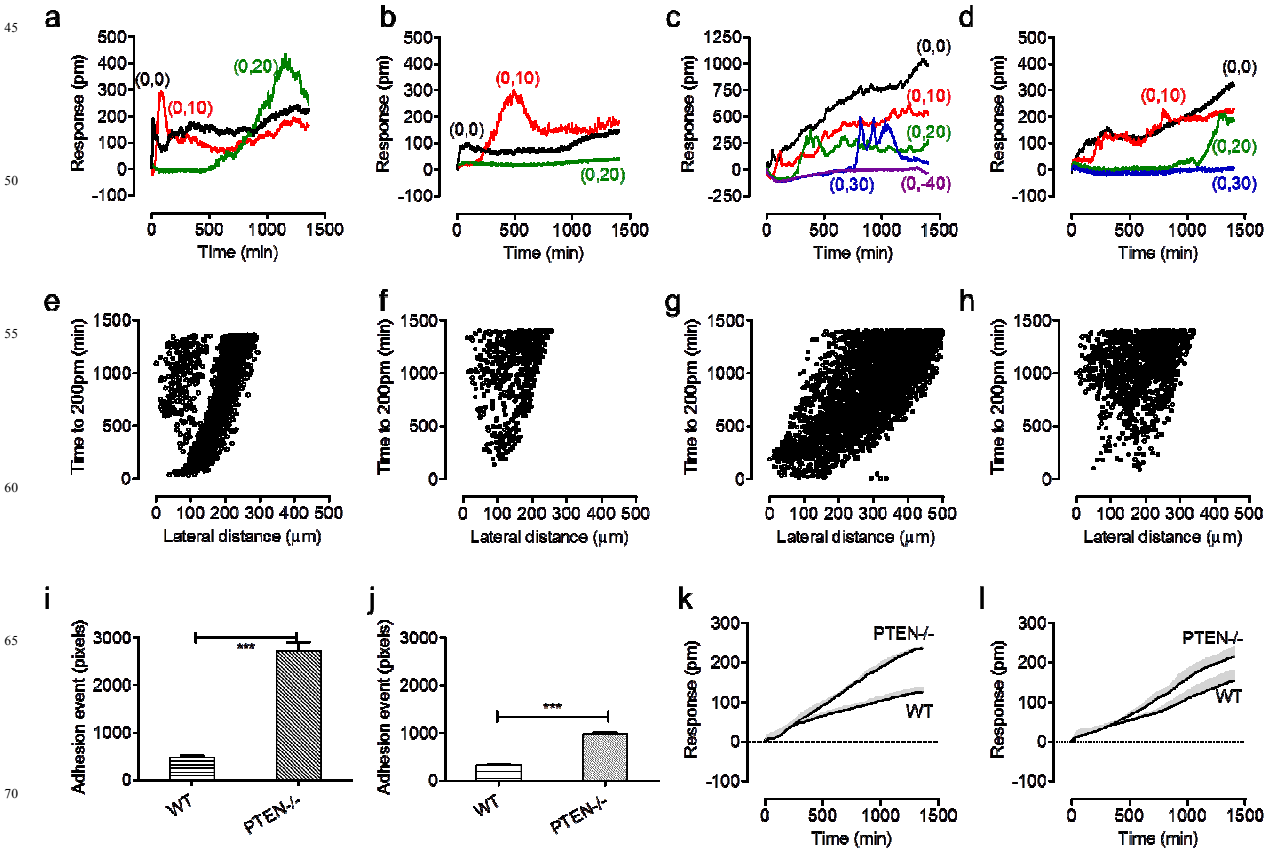

Fig. 5 PTEN deletion increases the invasion rate of CRC cells in spheroid through 3D Matrigel matrix. (a-d) The representative DMR of cells at specific pixels starting from the middle of the dot line to the right, as indicated in Supplementary Fig. S2e-h, respectively. (e-h) Correlation analysis between the adhesion time (that is, the time to reach 200pm DMR) and lateral distance. (a,e) The WT cells on the low density matrix; (b,f) the WT cells on the high density matrix; (c,g) the PTEN-/- cells on the low density matrix; (d,h) the PTEN-/- cells on the high density matrix. (i, j) The adhesion events *versus* cell types on the low (i) and high (j) density matrix. (k,l) The averaged DMR of both types of cells on the low (k) and high (l) density matrix. Low and high density matrix: 0.1mg/ml Matrigel and 0.2mg/ml Matrigel, respectively. WT, wide-type HCT116 cells; PTEN-/-, HCT116-PTEN-/- cells. Data represent mean±s.d. for i-l (n

View Article Online
DOI: 10.1039/C4IB00298A

= 3). *** p<0.001.

Correlation analysis showed that the parental cell line gave rise to an exponential increase in adhesion time over the increased distance for most adhesion events on the low density matrix surface (**Fig.5e**), but no clear correlation was found on the high density matrix surface (**Fig.5f**). Similar but clearer trend was observed for the PTEN-/- cells (comparing **Fig.5g** with **Fig.5h**). These results are best explained by the possibility that the 3D matrix acts as a microenvironment barrier to govern the invasion and adhesion path, and different mechanisms govern the invasion process when the matrix density is different. Both matrix metalloproteinase (MMP)-independent and dependent mechanisms can contribute to the invasion of cancer cells through the 3D matrix.[62-64] The MMP-independent invasion is sensitive to the pore size of the 3D matrix and the deformability of the cell nucleus, while the MMP-dependent mechanism requires the use of active invadopodia containing the cell surface MMPs to degrade the ECM and enlarge the matrix pore. The MMP-independent mechanism has been reported to be the main contributor to cell invasion in the low density 3D matrix,[63] consistent with our findings that the invasion rate of both cell lines on the low density gel appeared follow a simple exponential rule (**Fig.5e** and **Fig.5g**). Of note, PTEN knockout was shown to increase cell size.[65]

The single cell analysis further suggests that PTEN knockout increases the invasiveness of HCT116 cells. First, PTEN deletion increased the invasion distance (Comparing **Fig.5g** with **Fig.5e** on the low density matrix, or comparing **Fig.5h** with **Fig.5f** on the high density matrix). Second, PTEN deletion increased either the total adhesion events or the adhesion events in the end of assay on either the low density matrix (**Fig.5i**), or the high density matrix (**Fig.5j**). Third, PTEN deletion increases the kinetics and amplitude of the population averaged DMR on either the low density matrix (**Fig.5k**), or the high density matrix (**Fig.5l**).

Collectively, these results suggest that PTEN deletion increases the invasion speed of HCT116 cells in spheroid through 3D matrix at single cell level, and cell invasion mechanism is sensitive to the ECM density.

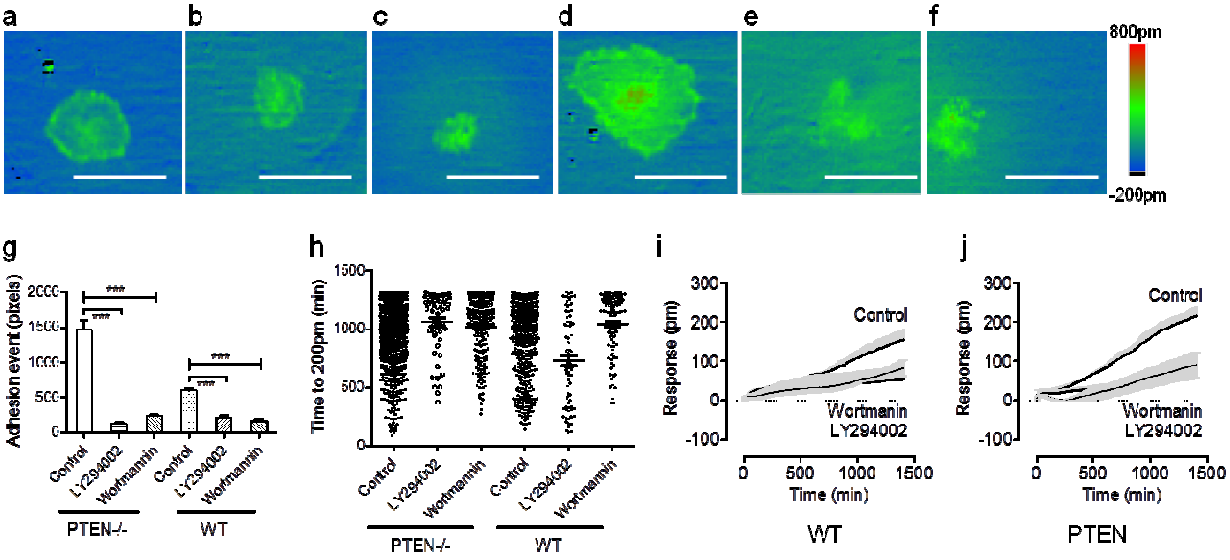

Fig. 6 The effect of PI3K inhibitors on the invasion profiles of CRC cells in spheroid through 3D Matrigel. (a-f) Representative DMR images at 24hrs under different conditions: (a-c) the spheroid of parental cells in the absence (a) and presence of LY294002 (b) and wortmannin (c); (d-f) the spheroid of PTEN-/- cells in the absence (d) and presence of LY294002 (e) and wortmannin (f). (g) The total adhesion events of the spheroid of the WT and PTEN-/- cells under different conditions. (h) The time to reach 200pm for the spheroid of the WT and PTEN-/- cells under different conditions. (i, j) The averaged DMR of the spheroid of the parental cell (i), and the PTEN-/- cell (j) under different conditions. 0.2mg/ml Matrigel coating was used. Both inhibitors were assayed at 2.5μM. Scale bar in a-f: 500μm. False colour bar in a-f: -200 to 800pm. Data represent mean±s.d. for g-j (n=3). *** p<0.001.

The invasion and adhesion of CRC cells in spheroid through 3D Matrigel is sensitive to PI3K inhibitors

Lastly, we examined the effect of two PI3K inhibitors, LY294002 and wortmannin, on the invasion and adhesion of CRC cells in spheroid through 3D matrix. Considering that the MMP-independent mechanism is mostly used for the cell invasion in the low density matrix, we used the high density Matrigel for this study. LY294002 is a small molecule reversible PI3K inhibitor and is less potent than wortmannin which is a steroid metabolite isolated from fungi since and an irreversible PI3K inhibitor.[66]

Real-time RWG imaging showed several distinct effects of PI3K inhibitors. First, both inhibitors clearly reduced the size of adhesion area 24hrs after the spheroid of either cell line was placed onto the top surface of the 3D matrix (**Fig.6a-f**). Second, both inhibitors reduced significantly the total adhesion events within 24hrs assays for both cell lines (**Fig.6g**). These results suggest that the invasion of both cell lines is sensitive to PI3K

View Article Online
DOI: 10.1039/C4IB00298A

inhibitors. This is expected. PI3K hyperactivation in cancer cells is known to increase the expression of MMPs such as MMP-2 and MMP-9, the key proteolytic enzyme to degrade the basement membrane;[67-69] and the parental HCT116 bears somatic activating mutant PI3KCA,[22] so both cell lines have dysregulated PI3K pathway activity. Third, both inhibitors also slowed down significantly the time to reach optimal DMR after invaded through the 3D matrix and adhered onto the sensor surface (**Fig.6h**). Fourth, both inhibitors not only decreased the kinetics, but also significantly suppressed the averaged DMR of both types of cells (**Fig.6i** and **Fig.6j**).

Together, these results suggest that PI3K inhibitors reduce the invasion and adhesion of HCT116 cells, and the invasion inhibitory activity of PI3K inhibitors is sensitive to the PTEN expression in HCT116 cells.

Conclusions

Motility and invasion are key hallmarks distinguishing benign from malignant tumours, offering a rich source of novel molecular targets for developing inhibitors to restrain both metastasis and angiogenesis. The PTEN-PI3K pathway is one of the most dysregulated pathways in many cancers including CRCs; however, little is known about the role of PTEN deletion on the invasion of multicellular CRC spheroids through 3D ECM matrix. On the other hand, 3D cancer cell models are increasingly recognized to be important for anti-cancer drug discovery due to their ability to recapitulate the *in vivo* properties of solid tumours; however, current assays to measure cell invasion in 3D matrix are cumbersome.

Here we used a recently developed label-free, real-time, single-cell and quantitative assay to measure the invasion of 3D spheroidal cells through 3D Matrigel with a goal to elucidate the effect and mechanisms of PTEN knockdown on the invasion process of CRC cells. Light microscopy imaging showed that PTEN knockout prevents the compaction and growth of large aggregates formed with high initial number of CRC cells. Through comparison of the 2D migration, Transwell invasion and single cell $3D^2$ invasion assay results for a pair of isogenic cell lines, wide-type and PTEN-/- HCT116 cells, we found that PTEN knockdown accelerates the 2D migration rate, the invasion rate in Transwell format, as well as the invasion speed of spheroidal cells through 3D Matrigel. In particular, the single cell real-time quantification using RWG biosensor imaging technique showed that PTEN knockout expedites cell dissociation from the spheroidal structure and adhesion onto the surfaces, the mechanisms governing cell invasion are sensitive to ECM matrix density, and the invasion inhibitory sensitivity of PI3K inhibitors is also sensitive to PTEN expression level. The present study presents evidence supporting the important role of PTEN knockout on the cancer invasion, and also highlights the great potential of label-free $3D^2$ invasion assay, in general label-free cell assays, for cancer research[70] and drug discovery.[71,72] Of note, label-free biosensors having long penetration depth, such as mid-infrared surface plasmon resonance[73] and multi-depth RWG biosensors[74], may offer additional insights for investigating cancer cell invasion in 3D environment.

Notes and references

[a] *Biochemical Technologies, Science and Technology Division, Corning Inc., Corning, NY 14831, United States of America*
[b] *S. Chandrasekaran was a summer intern at Corning Incorporated in 2014 when he performing most of assays described in this study. His present address: Department of Biomedical Engineering, Cornell University, Ithaca, New York, United States of America*
** Address correspondence to: Ye Fang, Fax: +1 607-974-5957. E-mail address: fangy2@corning.com.*

1 J, Li, *et al.* PTEN, a putative protein tyrosine phosphatase gene mutated in human brian, breast and prostate cancer. *Science* 1997, 275(5308), 1943-1947.
2 L. Salmena, A. Carracedo, P. P. Pandolfi, Tenets of PTEN tumor suppression. *Cell* 2008, 133(3), 403-414.
3 M. S. Song, L. Salmena, P. P. Pandolfi, The functions and regulation of the PTEN tumour suppressor. *Nat. Rev. Mol. Cell Biol.* 2012, 13(5), 283-296.
4 L. D. Wood, *et al.,* The genomic landscapes of human breast and colorectal cancers. *Science* 2007, **318**(5853), 1108-1113.
5 S. A. Danielsen, *et al.* Novel mutations of the suppressor gene PTEN in colorectal carcinomas stratified by microsatellite instability- and TP53 mutation-status. *Hum. Mutat.* 2008, **29**(11):E252-62.
6 A. Goel, *et al.,* Frequent inactivation of PTEN by promoter hypermethylation in microsatellite instability-high sporadic colorectal cancers. *Cancer Res.* 2004, 64(9), 3014-3021.
7 P.A. Laurent-Puig, *et al.,* Analysis of PTEN, BRAF, and EGFR status in determining benefit from cetuximab therapy in wild-type KRAS metastatic colon cancer. *J. Clin. Oncol.* 2009, 27(35), 5924-5930.
8 M. Frattini, *et al.,* PTEN loss of expression predicts cetuximab efficacy in metastatic colorectal cancer patients. *Br. J. Cancer* 2007, 97(8):1139-1145.
9 A. Naguib, *et al.*, Alterations in PTEN and PIK3CA in colorectal cancers in the EPIC Norfolk study: associations with clinicopathological and dietary factors. *BMC Cancer* 2011, **11**, 123.
10 P. G. Rychahou, *et al.,* Akt2 overexpression plays a critical role in the establishment of colorectal cancer metastasis. *Proc. Natl. Acad. Sci. USA* 2008, 105(51), 20315-20320.
11 T. Armaghany, *et al.,* Genetic alterations in colorectal cancer. *Gastrointest Cancer Res.* 2012, 5(1),19-27.
12 B. Weigelt, J. L. Peterse, L. J. van't Veer, Breast cancer metastasis: markers and models. *Nat. Rev. Cancer* 2005, 5(8), 591–602.
13 K. Pantel, R. H. Brakenhoff, Dissecting the metastatic cascade. *Nat Rev Cancer* 2004, 4(6), 448–456.
14 Y. Geng, J. R. Marshall, M. R. King, Glycomechanics of the metastatic cascade: tumor cell-endothelial cell interactions in the circulation. *Ann. Biomed. Eng.* 2012, 40(4), 790–805.
15 S. Valastyan, R. A. Weinberg, Tumor metastasis: molecular insights and evolving paradigms. *Cell* 2011, 147(2), 275-292.
16 D. Hanahan, R. A. Weinberg, Hallmarks of cancer: the next generation. *Cell* 2011, 144(5), 646–674.
17 B. Vogelstein, K. W. Kinzler, Cancer genes and the pathways they control. *Nat. Med.* 2004, 10(8), 789–799.
18 Y. Samuels, *et al.,* High frequency of mutations of the PI3KCA gene in human cancers. *Science* 2004, 304(5760), 554.
19 B. S. Jaiswal, *et al.,* Somatic mutations in p85α promote tumorigenesis through class IA PI3K activation. *Cancer Cell* 2009, 16(6), 463-474.
20 J. A. Engleman, J. Luo, L. C. Cantley, The evolution of phosphatidylinositol 3-kinases as regulators of growth and metabolism. *Nat. Rev. Genet.* 2006, 7(8), 606-619.
21 B. Vanhaesebroeck, I. Stephens, P. Hawkins, PI3K signalling: the path to discovery and understanding. *Nat. Rev. Mol. Cell Biol.* 2012, 13(3), 195-203.
22 Y. Samuels, *et al.,* Mutant PI3K3CA promotes cell growth and invasion of human cancer cells. *Cancer Cell* 2005, 7(6), 561-573.
23 K. A. Bowen, *et al.,* PTEN loss induces epithelial-mesenchymal transition in human colon cancer cells. *Anticancer Res.* 2009, 29(11), 4439-4449.

View Article Online
DOI: 10.1039/C4IB00298A

24 M.-J.- Langlois, *et al.,* The PTEN phosphatase controls intestinal epithelial cell polarity and barrier function: role in colorectal cancer progession. *PLoS One* 2010, 5(12), e15742.

25 A. Jeans, C. J. Gottardi, A. S. Yap, Cadherins and cancer: how does cadherin dysfunction promote tumor progression? *Oncogene* 2008, 27(55), 6920-6929.

26 F. Hirschhaeuser, *et al.,* Multicellular tumor spheroids: an underestimated tool is catching up again. *J. Biotechnol*. 2010, 148(1), 3–15.

27 M. Håkanson, M. Textor, M. Charnley, Engineered 3D environments to elucidate the effect of environmental parameters on drug response in cancer. *Integr. Biol.* 2011, 3(1), 31-38

28 A. R. Aref, *et al.,*Screening therapeutic EMT blocking agents in a three-dimensional microenvironment. *Integr. Biol.* 2013, 5(2), 381-389.

29 P.-A. Vidi, J. F. Leary, S. A. Lelièvre, Building risk-on-a-chip models to improve breast cancer risk assessment and prevention. *Integr. Biol.* 2013, 5(9), 1110-1118.

30 B. A. Justice, N. A. Badr, R. A. Felder, 3D cell culture opens new dimensions in cell-based assays. *Drug Discov. Today* 2009, 14(1-2), 102-107.

31 K. E. Chitcholtan, *et al.,* Differences in growth properties of endometrial cancer in three dimensional (3D) culture and 2D cell monolayer. *Exp. Cell Res.* 2013, 319(1), 75-87.

32 V. Härmä, *et al.,* A comprehensive panel of three-dimensional models for studies of prostate cancer growth, invasion and drug responses. *PLoS One* 2010, 5(5), e10431.

33 M. Pickl, C. H. Ries, Comparison of 3D and 2D tumor models reveals enhanced HER2 activation in 3D associated with an increased response to trastuzumab. *Oncogene* 2009, 28(3), 461–468.

34 A. C. Luca, *et al.,* Impact of the 3D microenvironment on phenotype, gene expression, and EGFR inhibition of colorectal cancer cell lines. *PLoS One* 2013, 8(3), e59689.

35 K. Lawrenson, *et al.,* Modelling genetic and clinical heterogeneity in epithelial ovarian cancers. *Carcinogenesis* 2011, 32(10), 1540-1549.

36 A. Busse, *et al.,* Characterization of small spheres derived from various solid tumor cell lines: are they suitable targets for T cells? *Clin. Exp. Metastasis* 2013, 30(6), 781-791.

37 M. W. Tibbitt, K. S. Anseth, Dynamic microenvironments: the fourth dimension. *Sci. Transl. Med.* 2012, 4(160), 160ps124.

38 N. Kramer, *et al.,* In vitro cell migration and invasion assays. *Mutat. Res*. 2013, 752(1), 10-24.

39 E. Kniazeva, A. J. Putnam, Endothelial cell traction and ECM density influence both capillary morphogenesis and maintenance in 3-D. *Am. J. Physiol. Cell Physiol.* 2009, 297(1), C179–C187.

40 S. Blacher, *et al.,* Cell invasion in the spheroid sprouting assay: a spatial organization analysis adaptable to cell behaviour. *PLoS One* 2014, 9(5), e97019.

41 S. Ghosh, *et al.,* Use of multicellular tumor spheroids to dissect endothelial cell–tumor cell interactions: a role for T-cadherin in tumor angiogenesis. *FEBS Lett.* 2007, 581(23), 4523–4528.

42 D. Oxmann, *et al.,* Endoglin expression in metastatic breast cancer cells enhances their invasive phenotype. *Oncogene* 2008, 27(25), 3567–3575.

43 F. Sabeh, R. Shimizu-Hirota, S. J. Weiss, Protease-dependent versus-independent cancer cell invasion programs: three-dimensional amoeboid movement revisited. *J. Cell Biol.* 2009, 185(1), 11–19.

44 N. K. Febles, A. M. Ferrie, Y. Fang, Label-free single cell quantification of the invasion of spheroidal colon cancer cells through 3D Matrigel. *Anal. Chem.* 2014, 86(17), 8842–8849.

45 M. Vinci, *et al.,* Advances in establishment and analysis of three-dimensional tumor spheroid-based functional assays for target validation and drug evaluation. *BMC Biol.* 2012, 10, 29.

46 A. M. Ferrie, *et al.,* High resolution resonant waveguide grating imager for cell cluster analysis under physiological condition. *Appl. Phys. Lett.* 2012, 100, 223701.

47 A. M. Ferrie, *et al.,* High frequency resonant waveguide grating imager for assessing drug-induced cardiotoxicity. *Appl. Phys. Lett.* 2014, 104, 183702.

48 Y. Fang, *et al.,* Characteristics of dynamic mass redistribution of EGF receptor signaling in living cells measured with label free optical biosensors. *Anal. Chem.* 2005, 77(17), 5720-5725.

49 Y. Fang, *et al.,* Resonant waveguide grating biosensor for living cell sensing. *Biophys. J.* 2006, 91(5), 1925-1940.

50 Y. Fang, A. M. Ferrie, Label-free optical biosensor for ligand-directed functional selectivity acting on β2-adrenoceptor in living cells. *FEBS Lett.* 2008, 582(5), 558–564.

51 F. Verrier, *et al.,* GPCRs regulate the assembly of a multienzyme complex for purine biosynthesis. *Nat. Chem. Biol.* 2011, 7(10), 909–915.

52 V. Goral, *et al.,* Agonist-directed desensitization of the β2-adrenergic receptor. *PLoS One* 2011, 6(4), e19282.

53 A. M. Ferrie, H. Sun, Y. Fang, Label-free integrative pharmacology on-target of drugs at the β2-adrenergic receptor. *Sci. Rep.* 2011, 1, 33.

54 H. Deng, *et al.,* Probing biochemical mechanisms of action of muscarinic M3 receptor antagonists with label-free whole-cell assays. *Anal. Chem.* 2012, 84(19), 8232−8239.

55 A. M. Ferrie, *et al.,* Label-free optical biosensor with microfluidics identifies an intracellular signalling wave mediated through the β2-adrerengic receptor. *Integr. Biol.* 2013, 5(10), 1253 - 1261.

56 H. Deng, *et al.,* Discovery of 2-(4-methylfuran-2(5H)-ylidene)malononitrile and thieno[3,2-b]thiophene-2-carboxylic acid derivatives as G protein-coupled receptor-35 (GPR35) agonists. *J. Med. Chem.* 2011, 54, 7385–7396.

57 G. Benton, *et al.,* Multiple uses of basement membrane-like matrix (BME/Matrigel) in vitro and in vivo with tumor cells. *Intl. J. Cancer* 2011, 128(8), 1751–1757.

58 C.-C. Liang, A. Y. Park, J.-L. Guan, In vitro scratch assay: a convenient and inexpensive method for analysis of cell migration in vitro. *Nat. Protoc.* 2007, 2(2), 329–333.

59 C. Lee, J. S. Kim, T. Waldman, PTEN gene targeting reveals a radiation-induced size checkpoint in human cancer cells. *Cancer Res.* 2004, 64(19), 6906-6914.

60 J. Z. Zhang, *et al.,* The use of spectroscopic imaging and mapping techniques in the characterisation and study of DLD-1 cell spheroid tumour models. *Integr. Biol.* 2012,4(9), 1072-1080.

61 R. W. Kasinskas, R. Venkatasubramanian, N. S. Forbes, Rapid uptake of glucose and lactate, and not hypoxia, induces apoptosis in three-dimensional tumor tissue culture. *Integr. Biol.* 2014, 6(4), 399-410.

62 Y. Wang, M. A. McNiven, Invasive matrix degradation at focal adhesions occurs via protease recruitment by a FAK–p130Cas complex. *J. Cell Biol.* 2012, 196(3), 375-385.

63 K. Wolf, *et al.,* Physical limits of cell migration: Control by ECM space and nuclear deformation and tuning by proteolysis and traction force. *J. Cell Biol.* 2013, 201(7), 1069-1084.

64 A. Pathak, S. Kumar, Biophysical regulation of tumor cell invasion: moving beyond matrix stiffness. *Integr. Biol.* 2011, 3(4), 267-278.

65 J. S. Kim, *et al.,* Mechanistic analysis of a DNA damage-induced, PTEN-dependent size checkpoint in human cells. *Mol. Cell Biol.* 2011, 31(13), 2756-2771.

66 D. Kong, T. Yamori, Phosphatidylinositol 3-kinase inhibitors: promising drug candidates for cancer therapy. *Cancer Sci.* 2008, 99(9), 1734-1470.

67 S. Shukla, *et al.,* Activation of PI3K-Akt signaling pathway promotes prostate cancer cell invasion. *Int. J. Cancer* 2007, 121(7), 1424-1432.

68 J. Chen, *et al.,* Involvement of PI3K/PTEN/AKT/mTOR pathway in invasion and metastasis in hepatocellular carcinoma: Association with MMP-9. *Hepatol. Res*. 2009, 39(2), 177–186.

69 Y. Yin, W. H. Shen, PTEN: a new guardian of the genome. *Oncogene* 2008, 27(41), 5443–5453.

70 Y. Fang, Probing cancer signaling with resonant waveguide grating biosensors. *Exp. Opin. Drug Discov.* 2010, 5(12), 1237-1248.

71 Y. Fang, Troubleshooting and deconvoluting label-free cell phenotypic assays in drug discovery. *J. Pharmacol. Tox. Methods* 2013, 67(2), 69-81.

72 Y. Fang, Label-free drug discovery. *Front. Pharmacol.* 2014, 5, 52.

73 V. Yashunsky, *et al.,* Real-time monitoring of epithelial cell-cell and cell-substrate interactions by infrared surface plasmon spectroscopy. *Biophys. J.* 2010, 99(12), 4028-4036.

View Article Online
DOI: 10.1039/C4IB00298A

74 R. Horvath, *et al.,* Multidepth screening of living cells using optical waveguides. *Biosens. Bioelectron*. 2008, 24(4), 805-810.

View Article Online
DOI: 10.1039/C4IB00298A

Scheme

Label-free single cell 3D^2 invasion assay enables real-time quantification of the invasion of spheroidal cells through 3D Matrigel and provides insights for the role of PTEN in colorectal cancer cell invasion.